FLOW DEVELOPMENT OF A GAS-SOLID SUSPENSION IN A MICROGRAVITY COUETTE APPARATUS

Haitao Xu and Michel Y. Louge
Sibley School of Mechanical and Aerospace Engineering, Cornell University, Ithaca, NY 14853, USA

and James T. Jenkins
Department of Theoretical and Applied Mechanics, Cornell University, Ithaca, NY 14853, USA

ABSTRACT

We analyze the development of a gas-solid flow in an axisymmetric shear cell without gravitational accelerations. A gas pressure gradient imposed on the cell induces a relative motion between the two phases, while the differential rotation of the cell boundaries allows the independent control of the solids agitation. We model variations of the cross-sectional averaged solid volume fraction, mean velocity and fluctuation energy along the cell using a technique similar to the integral treatment of a boundary layer. The theory finds a condition for which fully-developed flows can be achieved in regions of the cell.

INTRODUCTION

Gas-solid flows are widely encountered in industry and in nature. An appreciation has recently developed for the importance of collisional interactions among particles in these flows[1,2]. Koch, Sangani and their co-workers consider the contribution of the viscous forces of the gas to both the dissipation[3] and the production[4] of particle fluctuation energy in gas-particle systems. To test their theories, we are designing a microgravity Couette cell in which to study the interaction of a flowing gas with relatively massive particles that collide with each other and with the moving boundaries of the cell.

In a first series of experiments[5], we will study the viscous dissipation of the particle fluctuation energy when there is no relative mean velocity between gas and solids. In this case, the gas-particle flow in the Couette cell will be steady and fully-developed everywhere by symmetry. In a second series of experiments, we will impose a gas pressure gradient on the cell to create a relative mean motion between gas and solids. Here, the objective is to study the effect of particle fluctuation on the drag coefficient. Because the imposed pressure gradient breaks down the symmetry of these experiments, the gas-solid flows must develop along the cell.

To predict this development, we follow a procedure similar to that of Xu et al[6]. Starting with the kinetic theory of Jenkins and Richman[7], Xu et al capture the variations of the mean solid volume fraction, granular temperature and velocity of colliding grains along the straight channel of a shear cell using a one-dimensional analysis analogous to the integral treatment of laminar boundary layers.

In this paper, we extend the theory of Xu et al to gas-solid flows by coupling the gas and solid momentum balances and by including effects of viscous dissipation in the balance equation of particle fluctuation energy. We then integrate these equations numerically to find the evolution equations of particle volume fraction, granular temperature and gas pressure. To illustrate the results, we present a set of conditions for which the experiment features regions of fully-developed flow.

EXPERIMENTAL SETUP

In our experiments, three small distributor plates exchange gas with the Couette cell, thus dividing the latter into three regions (Fig. 1). The rotation of the inner bumpy boundary creates a mean counter-clockwise motion of particles in the cell. In the "co-flow" region, the gas pressure gradient entrains the solids. In the "counter-flow" region, particles are decelerated by the streamwise pressure gradient in the gas.

In the third region, the gradient is made to vanish by supplying an appropriate amount of gas through the third distributor (Fig. 1), thus equalizing the gas and solid velocities through most of the channel cross-section, except in narrow regions near the moving boundaries and the flat side walls. The purpose of this region of low drag is to infer the volume flow rate of gas from measurements of the velocity and volume fraction of solids. Particle velocities are measured

through the side walls using the computer tracking technique of Louge, et al[8]; the solid volume fraction is recorded by a capacitance instrument[9]. Simple balances then permit us to calculate the mass flow rate of gas through all three channel regions from measurements of the corresponding quantities supplied to the two inlet distributors.

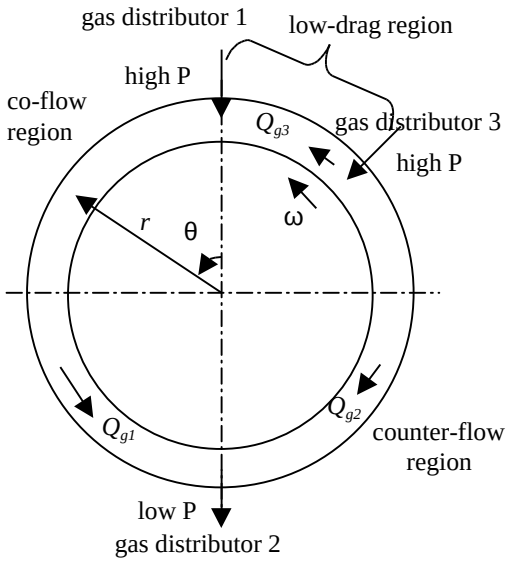

Figure 1. Sketch of the Couette cell. Arrows in the channel indicate the directions of gas flow. The inner boundary of the cell rotates at the angular velocity ω. Gas volume flow rates in three regions are Q_{g1}, Q_{g2} and Q_{g3}, respectively.

In current design, because the third gas distributor is located only π/4 radians away from the first, we expect that the co-flow and counter-flow regions will both feature a fully-developed quadrant long enough to compare experimental measurements of particle velocity and granular temperature to theoretical predictions. The purpose of our present analysis is to confirm this expectation.

In this paper, the inner and outer radii of the flow channel are R_i and R_o, respectively; $R=(R_i+R_o)/2$ is the radius at the channel centerline, $H=R_o-R_i$ is the width of the channel, θ is the azimuth incremented along the direction of motion of the inner boundary, and r and z are the radial and depth coordinates, respectively. Because $H<<R$ in the current design, we neglect the effect of centripetal acceleration in our analysis.

GOVERNING EQUATIONS

We consider the motion of a gas-particle system in the absence of gravity. For the solid phase, we use the conservation equations derived by Jenkins and Richman[7], to which we add a drag force in the momentum balance and a viscous dissipation term in the balance of particle fluctuation energy. In a steady flow the resulting equations are:

$$(\rho \mathbf{u}) = 0 \tag{1}$$

$$(\rho \mathbf{uu}) = -\left[N - \kappa(\quad \mathbf{u})\right] + \quad \tau + \beta(\mathbf{v} - \mathbf{u}) \tag{2}$$

$$\left[(3/2)\rho \mathbf{u} T\right] = -\quad \mathbf{q} - D_{inelas} - D_{viscous} + \left\{\left[-N + \kappa(\quad \mathbf{u})\right]\mathbf{I} + \tau\right\} : \mathbf{S} \tag{3}$$

where $\rho=\varphi\rho_s$ is the bulk density; φ is the solid volume fraction; ρ_s is the material density of the grains; **u** and **v** are the mean velocity of solid and gas phase, respectively; β is a drag coefficient that incorporates the buoyancy force associated with the gas pressure gradient; and **I** is the identity tensor. The shear stress tensor of solid phase is $\tau = 2\mu\hat{\mathbf{S}}$, where μ is the shear viscosity and $\hat{\mathbf{S}}$ is the deviatoric part of the symmetric velocity gradient $\mathbf{S} = (1/2)\left[(\quad \mathbf{u}) + (\quad \mathbf{u})^T\right]$. The heat flux is $\mathbf{q} = -k\quad T$ and N, κ, and k are the solid phase pressure, bulk viscosity, and heat conductivity rate, respectively. The granular temperature is $T \equiv \langle C^2 \rangle / 3$, where C is the fluctuation velocity. D_{inelas} and $D_{viscous}$ are the volumetric rates of dissipation of granular fluctuation energy due, respectively, to the inelasticity of the particles and the viscous interactions with the gas.

In our experiments with agitated, massive metal spheres immersed in a gas of ordinary viscosity (air or nitrogen), the gas shear stress at the walls is negligible and the gas pressure gradient is mainly balanced by the drag force between gas and solids except when solid volume fractions are very low. In addition, because the particle Reynolds number is small in all experimental conditions, the gas inertia can also be neglected in the momentum balance. Hence, the governing equations for the gas reduce to:

$$\left[(1-\varphi)\mathbf{v}\right] = 0 \tag{4}$$

and

$$p = \beta(\mathbf{u}-\mathbf{v}) \tag{5}$$

where p is the gas pressure.

Jenkins and Richman[7] derive the following constitutive relations from the kinetic theory,

$$N = \rho T(1+4G) \tag{6}$$

$$\kappa = \left(8/3\sqrt{\pi}\right)\rho d T^{1/2} G \tag{7}$$

$$\mu = \left(8J/5\sqrt{\pi}\right)\rho d T^{1/2} G \tag{8}$$

$$k = \left(4M/\sqrt{\pi}\right)\rho d T^{1/2} G \tag{9}$$

$$D_{inelas} = \left(24/d\sqrt{\pi}\right)\left(1-e_{eff}\right)\rho T^{3/2} G \tag{10}$$

where d is the diameter of grains, and G, J, and M are known functions of φ. The effective coefficient of normal restitution e_{eff} captures frictional energy losses in the flow[10].

Sangani et al[3] propose the following form for the viscous dissipation based on their numerical simulations:

$$D_{viscous} = 54\varphi\mu_g T R_{diss}/d^2 . \tag{11}$$

where μ_g is the gas viscosity, $R_{diss}(\varphi)$ is a known function of solid volume fraction and the ratio of the gas mean free path to the particle diameter. For the drag, we borrow the coefficient that Koch and Sangani[4] used for sedimentation:

$$\beta = 18\mu_g\varphi(1-\varphi)R_{drag}/d^2 \tag{12}$$

where $R_{drag}(\varphi)$ is derived from numerical simulations.

FLOW DEVELOPMENT MODEL

We consider the gas-particle flow in the axisymmetric cell sketched in Figure 1. The channel is bound by an inner moving wall of speed $U=\omega R_i$ to which cylindrical bumps are affixed, by a stationary bumpy outer wall, and by two flat side walls. Our one-dimensional analysis focuses on the streamwise variations of volume fraction, velocity and temperature averaged through the channel cross-section, where the cross-sectional average of a flow quantity ψ is defined as:

$$\overline{\psi} \equiv \frac{1}{HW}\int_{R_i}^{R_o}\int_{-W/2}^{W/2}\psi(r,z)\,dz\,dr , \tag{13}$$

and W is the depth of the flow channel.

In a study of the development of a collisional granular flow along a straight channel with similar boundary features, Xu et al[6] made these integrations tractable by assuming that:

(1) The granular temperature and solid volume fraction are uniform in any cross section, i.e., $T=T(\theta)$, $\varphi=\varphi(\theta)$.

(2) The velocity component vanishes in z-direction and other components are independent of z, i.e., $\mathbf{u}=(u_r(\theta,r),\, u_\theta(\theta,r),\, 0)$.

(3) Because $H<<R$, $(1/r)(\partial u_r/\partial\theta) << \partial u_\theta/\partial r$.

(4) At each section, u_θ has the form of the fully developed profile in absence of centripetal acceleration, i.e., the transverse profile of u_θ at an arbitrary cross-section of angular position θ is:

$$u_\theta(\theta,r) = \bar{u}(\theta) + u_{sh}\eta \tag{14}$$

where $\eta\equiv(r-R)/H$ is the dimensionless coordinate in r-direction and u_{sh} is a constant. This assumption allows u_{sh} to be derived from solutions of the fully-developed flow.

(5) The shear stress $\tau_{\theta z}$ is proportional to z and vanishes at the center plane by symmetry, i.e.,

$$\tau_{\theta z} = \frac{2z}{W}\tau_{sw}, \quad (-W/2 \le z \le W/2), \tag{15}$$

where τ_{sw} is the shear stress at the flat side walls.

(6) All collisions between flow spheres and flat side walls are "sliding"[11]. Although this assumption is not essential, it simplifies the calculation of shear stresses and heat fluxes at the flat side walls.

Note that although we assume $\partial T/\partial z=0$ and $\partial u_\theta/\partial z=0$, we retain the heat fluxes and shear stresses on surfaces normal to z to capture the effects of side walls when we integrate the energy and momentum equations. Similarly, we retain the heat fluxes on the inner and outer bumpy walls despite assuming $\partial T/\partial r=0$.

We integrate the momentum and energy equations in r- and z-direction to find the evolution of $\bar{u}$, φ and T along θ. At the flat side walls, we use the boundary conditions derived by Jenkins[11] and Jenkins & Louge[12] to evaluate the shear stress and heat flux at the wall,

respectively; at the bumpy boundaries, we use the nonlinear boundary conditions derived by Jenkins et al[13]. These boundary conditions have the functional form:

$$\tau_w / N = f_\tau(u_{slip}, T, \varphi, \mu_w) \tag{16}$$

$$q_w / \left(NT^{1/2}\right) = f_q(u_{slip}, T, \varphi, \mu_w, e_w) \tag{17}$$

where τ_w and q_w are, respectively, the shear stress and heat flux at the boundary; u_{slip} is the slip velocity there (i.e., the difference between wall velocity and the mean velocity of particles adjacent to the wall), and e_w and μ_w are the coefficient of restitution and friction of the wall, respectively. Equations (16) and (17) capture geometrical details of the bumpy boundaries and flat side walls.

After evaluating the integrals and using the boundary conditions, we obtain

$$\varphi\bar{u} = Q_s = const \tag{18}$$

$$\frac{d}{Rd\theta}\left(\frac{KQ_s}{\rho_s\varphi^2}\frac{d\varphi}{Rd\theta}\right) + \rho_s\left(\frac{u_{sh}^2}{12} - \bar{u}^2\right)\frac{d\varphi}{Rd\theta} + \frac{dN}{Rd\theta} - \frac{\tau_{yi} - \tau_{yo}}{H} + \frac{2\tau_{sw}}{W} + \beta(\bar{u} - \bar{v}) = 0, \tag{19}$$

$$\frac{d}{Rd\theta}\left(k\frac{dT}{Rd\theta}\right) - \frac{3}{2}\rho\bar{u}\frac{dT}{Rd\theta} + \frac{q_{yi} + q_{yo}}{H} + \frac{2q_{sw}}{W} + \frac{\mu}{H^2}u_{sh}^2 + \frac{\tau_{sw}^2}{3\mu} - D_{inelas} - D_{viscous} - N\frac{d\bar{u}}{Rd\theta} + K\left(1 + \frac{1}{12}\frac{u_{sh}^2}{\bar{u}^2}\right)\left(\frac{d\bar{u}}{Rd\theta}\right)^2 = 0, \tag{20}$$

$$(1-\varphi)\bar{v} = Q_g = const \tag{21}$$

and

$$\frac{dp}{Rd\theta} = \beta(\bar{u} - \bar{v}) \tag{22}$$

where $K \equiv \kappa + 4\mu/3$, Q_s and Q_g are the volume flow rates of solids and gas, respectively. In these equations, the shear stresses τ_{yi} and τ_{yo} at the top and bottom bumpy boundaries, the shear stress τ_{sw} at the flat side wall, and the heat fluxes through the top and bottom bumpy boundaries and the flat side walls q_{yi}, q_{yo} and q_{sw} are given in terms of T, φ and impact parameters by Eqs (16) and (17). In these one-dimensional equations, we further employ the mass conservation equation (18) and the equation of state (6) to eliminate $\bar{u}$ and N, respectively, in terms of volume fraction and temperature.

PERIODIC CONDITIONS

Equations (19), (20) and (22) are ordinary differential equations for the evolution of solid volume fraction, granular temperature and gas pressure. They are coupled through transport coefficients, the drag force and the viscous dissipation term. They are valid in each of the three regions shown in Fig 1. The gas pressure is known at the interface of any two regions. We further assume that the solid volume fraction, the granular temperature and their first order derivatives are continuous at the interfaces, i.e.,

$$\psi\left(\theta = \theta_i^-\right) = \psi\left(\theta = \theta_i^+\right), \tag{23}$$

$$\frac{d\psi}{Rd\theta}\left(\theta = \theta_i^-\right) = \frac{d\psi}{Rd\theta}\left(\theta = \theta_i^+\right), \tag{24}$$

where $\psi=\varphi$ or T, and the index i=1,2,3 represents the three distributors.

Note that because we ignore the inertia and viscous shear stress terms in the gas momentum equation, the gas velocity is not continuous along the cell. This implies a discontinuous drag force at the three distributors.

For given experimental conditions, Eqs (19), (20) and (22) are solved numerically with an initial guess for the volume flow rates of solid and gas. Note that while the solids volume flow rate is unique along the cell, its counterpart in the gas is different in each of the three regions. The solution yields the total mass of solid in the cell and the pressure difference across each of the three regions. The volume flow rates of solids and gas are then adjusted until these quantities i.e., the total mass of solid in the cell and the pressure difference across each of the three regions, converge on the values imposed in each experiment. Because of the non-linearity of the problem, we use a modified Newton-chord method[14] to carry out the corresponding iterations.

RESULTS AND DISCUSSION

Figure 2 to 4 show the development of a typical experiment. Here, the particles are 2 mm Nitinol spheres with a material density of 6.71 g/cm^3. The inner and outer boundaries are made of cylindrical bumps of 2mm diameter. The inner boundary rotates at 1.6 rad/s while the outer boundary remains stationary. The gas pressure at distributors 1 and 3 are 11.4 Pa higher than at distributor 2. The gas is air near standard conditions.

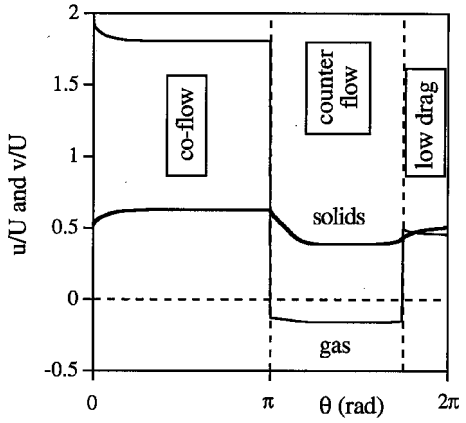

Figure 2. Predicted average solid and gas velocity along the cell, made dimensionless with the speed of the moving boundary. Gas distributors 1, 2 and 3 are located at θ=0, π and 7π/4, respectively.

Figure 2 shows the predicted average particle velocity and gas velocity along the cell. As expected, the gas moves faster than the solids in the co-flow region and, under these conditions, the gas and solid velocities point to opposite directions in the counter-flow region. Therefore, gas is admitted into the cell through both distributors 1 and 3 and it is withdrawn from distributor 2.

The gas and particle velocities are nearly undistinguishable throughout the region of low drag. Thus, it should be possible to infer the gas volume flow rates in all regions from measurements of solid velocity and volume fraction between distributors 1 and 3.

In Fig. 3, we note that the disturbance of the solid volume fraction arising from distributors 1 and 3 propagates upstream. Xu et al[6] observed this phenomenon in their computer simulations of collisional granular flows in a race track shear cell. Their one-dimensional model of flow development attributed this effect to the first term of Eq. (19), which depends crucially on the bulk and shear viscosities of the solid phase.

As Figs. 2 to 4 indicate, the gas pressure gradient is almost linear in the co-flow and counter-flow regions, and the volume fraction and velocities reach a wide plateau there. Therefore, we anticipate that these experimental conditions will permit us to reach a fully-developed state.

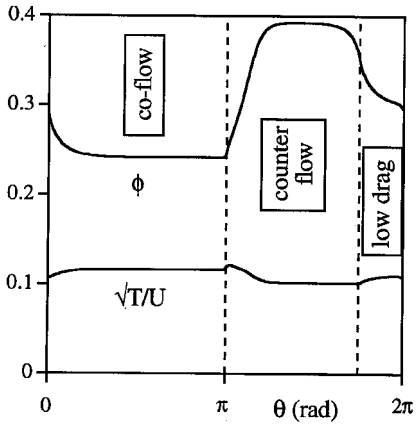

Figure 3. Predicted solid volume fraction and particle fluctuation velocity, made dimensionless with the speed of the moving boundary, along the cell. The impact properties of the particles are: coefficient of restitution =0.9, frictional coefficient = 0.1 and coefficient of tangential restitution = 0.4.

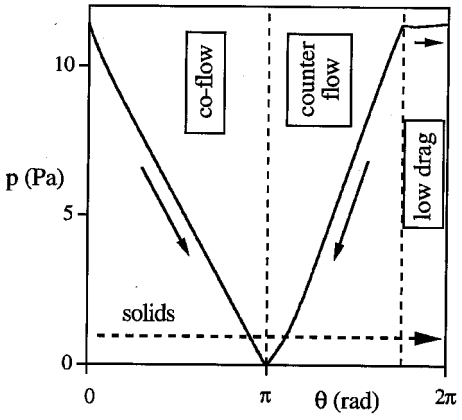

Figure 4. Predicted gas pressure along the cell. The solid arrows indicate the direction of the gas flow while the dashed arrow indicates the direction of solid flow.

ACKNOWLEDGEMENTS

This work was supported by NASA grants NCC3-468 and NAG3-2112 and by the International Fine Particle Research Institute.

REFERENCE

1. Sinclair, J.L. & Jackson, R. 1989 Gas-particle flow in a vertical pipe with particle-particle interactions. AIChE J. 39, 1473-1486.
2. Louge, M.Y., Mastorakos, M. & Jenkins J.T. 1991 The role of particle collisions in pneumatic transport. J. Fluid Mech. 231, 345-359.
3. Sangani, A.S., Mo, G., Tsao, H.-K. & Koch, D.L. 1996 Simple shear flows of dense gas-solid suspensions at finite Stokes number. J. Fluid Mech. 313, 309-341.
4. Koch, D.L. & Sangani, A.S. 1999 Particle pressure and marginal stability limits for a homogeneous monodisperse gas fluidized bed:kinetic theory and numerical simulations. J. Fluid Mech. 400, 229-263.
5. Louge, M.Y., Xu, H. & Jenkins, J.T. 2001 Studies of gas-particle interactions in a microgravity flow cell. In Powders and Grains 2001 (ed. Kishino, Y.), pp.557-560. Swets & Zeitlinger Publishers.
6. Xu, H., Louge, M.Y. and Jenkins, J.T., Flow development of a shearing collisional granular flow. In Powders and Grains 2001 (ed. Kishino, Y.), pp.359-362. Swets & Zeitlinger Publishers.
7. Jenkins, J.T. & Richman, M.W. 1985 Grad's 13-moment system for a dense gas of inelastic spheres. Arch. Rat. Mech. Anal. 87, 355-377.
8. Louge, M.Y., Jenkins, J.T., Reeves, A. & Keast, S. 2000 Microgravity segregation in collisional granular shearing flows. In IUTAM symposium on segregation in granular flows (ed. Rosato, A.D. & Blackmore, D.L.), pp.103-112. Kluwer Academic Publishers.
9. Louge, M., Tuccio, M., Lander, E. & Connors, P. 1996 Capacitance measurements of the volume fraction and velocity of dielectric solids near a grounded wall. Rev. Sci. Instrum. 67, 1869-1877.
10. Zhang, C. 1993 Kinetic theory for rapid granular flows. Ph.D Thesis. Cornell University.
11. Jenkins, J.T. 1992 Boundary conditions for rapid granular flows: flat frictional walls. J. Applied Mech. 59, 120-127.
12. Jenkins, J.T. & Louge, M.Y. 1997 On the flux of fluctuation energy in a collisional grain flow at a flat frictional wall, Phys. Fluids 9, 2835-2840.
13. Jenkins, J.T., Miyagchilov, Y. & Xu, H. 2000 Nonlinear boundary conditions for collisional grain flows. In preparation.
14. Ortega, J.M. & Rheinboldt, W.C. 1970 Iterative solution of nonlinear equations in several variables. New York: Academic Press.